

TEHD lubrication of a cylindrical and elliptical bearing two lobes "parametric study"

Aziz OUADOUD

Abstract— In this article, the thermoelastohydrodynamic study for the analysis of cylindrical and elliptical bearing (two-lobe) with a Newtonian lubricant was presented. The thermoelastic deformations of the solid parts are taken into account. To solve the Reynold's equation generalized, equation of energy and the displacement field, respectively, using two numerical techniques Computational Fluid Dynamic "CFD" and Fluid Structure Interaction "FSI". This article will aim to compare a cylindrical and elliptical bearing with two lobes. This comparison will focus on the various operating parameters of a bearing (pressure, temperature, displacement and stress) for different values of speed and eccentricity.

Index Terms— Thermoelastohydrodynamic, Cylindrical Elliptical journal bearing, Two-lobe.

I. INTRODUCTION

In the literature, we examined the simple case of cylindrical bearing, in practice, other bearing types are often used as the cylindrical bearing is stable only for large eccentricities, that is to say high loads. Another type of fixed geometry bearing and has good dynamic characteristics is the lobed bearing. Its configuration is similar to that of the tilt pad bearing, except that the pads (lobes) are fixed in a given position beforehand. If the tip is angled so that the minimum thickness of the film is located at the outlet of this lobe, while the converging zone and the lifts are increased. The basic principle of non-circular bearing is to make changes in the symmetry of a plain bearing, which encourages the characteristics of self-excited vibration, and overcome the adverse effects of the configuration of circular rotation. To combat the dynamic instability of rotating at high speed in their bearing trees is often chosen non-circular plain bearings. Among these, the elliptical bearing has a certain predilection. 2007 K Prabhakaran and all [2] showed static and dynamic analysis of behavior "EHD" an elliptical bearing (two lobes) with the use of two types of Newtonian lubricant and microfleece. The finite element method is used to solve the modified Reynolds equation and the equations of three-dimensional elasticity directing the displacement field in the bearing. The static and dynamic behavior characteristics are calculated for a wide range of deformation coefficient that takes into account the flexibility of the bearing. The calculated results show that increasing the concentration of additive volume and mass transfer additive produced significant on the performance characteristics of the bearing change. Amit Chauhan et al in

2010 [3], conducted a study "THD" parameter for the analysis of behaviors of an elliptical bearing lubricant for three different category. The finite difference method was adopted for the numerical solution of the generalized Reynolds equation and the energy in the lubricant film. Vikas Phalle, Satish C. Sharma and SC Jain [4] (2011), in this work the authors present an analytical study on the influence of wear on the performance of an offset two-lobe membrane four a hydrodynamic bearing pockets. The generalized Reynolds equation governing the flow of lubricant in the clearance space of a bearing system was solved using finite element method with Newton-Raphson. The numerically simulated results clearly indicate that the performance of the bearing is largely affected by wear.

II. EQUATIONS OF THE PROBLEM TEHD

A. Lubricant film thickness

For an elliptical bearing the lubricant film thickness is written as follows [3]:

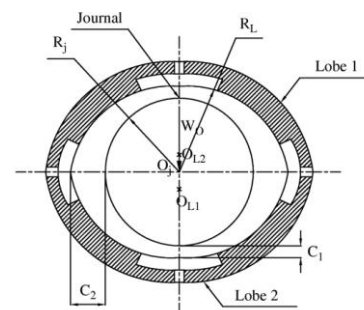


Figure1: Schematic elliptical journal bearing [3]

$$\begin{cases} h = C_m \{1 + E_m + \varepsilon_1 \cos(\theta + \phi - \phi_1)\} & 0^\circ \leq \theta \leq 180^\circ \\ h = C_m \{1 + E_m + \varepsilon_2 \cos(\theta + \phi - \phi_2)\} & 180^\circ \leq \theta \leq 360^\circ \end{cases} \quad (1)$$

Different parameters in equations (1) are given as

$$\varepsilon_1 = \sqrt{E_m^2 + \varepsilon^2 - 2E_m \varepsilon \cos(\phi)} ;$$

$$\varepsilon_2 = \sqrt{E_m^2 + \varepsilon^2 + 2E_m \varepsilon \cos(\phi)}$$

$$\phi_1 = \pi - \tan^{-1} \left(\frac{\varepsilon \sin(\phi)}{E_m - \varepsilon \cos(\phi)} \right) ;$$

$$\phi_2 = \tan^{-1} \left(\frac{\varepsilon \sin(\phi)}{E_m - \varepsilon \cos(\phi)} \right) ; \quad E_m \frac{C_h - C_m}{C_m}$$

Manuscript received September 23, 2014.

Pr. OUADOUD Aziz, Department of Physics, University Abdelmalek Essaadi/ Faculty Poly-disciplinary/multidisciplinary Laboratory, Larache, Morocco, Phone/+212 661604110.

B. Reynold's equation

The study of the lubrication of a bearing requires the application of various assumptions about mechanical viscous thin films. Assuming the fixed bearing and the shaft of a lively angular velocity ω , writing this equation in a Cartesian coordinate system leads to the following formula [5]:

$$\frac{\partial}{\partial \theta} \left(\frac{h^3}{12\mu} \frac{\partial P}{\partial \theta} \right) + R^2 \frac{\partial}{\partial z} \left(\frac{h^3}{12\mu} \frac{\partial P}{\partial z} \right) = \frac{UR}{2} \frac{\partial h}{\partial \theta} + \frac{V}{R^2} + \frac{h}{2R^2} \frac{\partial U}{\partial \theta} \frac{\partial h}{\partial t}$$

The boundary conditions on the pressure are quite simple: it is assumed that the reference pressure is atmospheric pressure. The pressure in the inlet sections and outlet of the film is considered equal to the supply pressure and the bearing edges of equal to atmospheric pressure.

C. Energy equation

The energy equation in mechanics of viscous thin films is a particular form of shape differs from an author to another depending on changes made to it. The energy equation written for an incompressible Newtonian fluid and the simplified calculation domain as follows.

$$\underbrace{\rho C_p \left[\frac{\partial T}{\partial t} + u \frac{\partial T}{\partial x} + v \frac{\partial T}{\partial y} + w \frac{\partial T}{\partial z} \right]}_{\text{Convection}} = \underbrace{K_h \frac{\partial^2 T}{\partial y^2}}_{\text{Conduction}} + \underbrace{\mu \left[\left(\frac{\partial u}{\partial y} \right)^2 + \left(\frac{\partial w}{\partial y} \right)^2 \right]}_{\text{Viscous dissipation}} \quad (3)$$

(u, v, w): Component of velocity,
 μ : Dynamic viscosity of lubricant;
 C_p : Specific heat of lubricant,
 K_h : Conduction coefficient.

D. Displacement equation

The equations governing the displacement field are given as:

$$[M_s] \{ \ddot{U} \} + [K_s] \{ U \} = [F_s] + [R] \{ P \} \quad (4)$$

$$\begin{bmatrix} M_s & 0 \\ \rho RT M_f \end{bmatrix} \begin{Bmatrix} \ddot{U} \\ \ddot{P} \end{Bmatrix} + \begin{bmatrix} K_s & -R_s \\ 0 & K_f \end{bmatrix} \begin{Bmatrix} U \\ P \end{Bmatrix} = \begin{Bmatrix} F_s \\ F_f \end{Bmatrix} \quad (5)$$

Where, $[M_s]$ is the structural mass matrix; $[M_f]$ is the fluid mass matrix; $[F_s]$ and $[F_f]$ is the structural and fluid force matrix; $[R]$ is a coupling matrix that represents the effective surface area associated with each node in fluid structure interface. The interaction of the fluid and the structure at the mesh interface causes the pressure to exert a force applied to the structure and the structural motions produce an effective "fluid load".

III. RESULTS AND DISCUSSIONS

The example given relates to a landing with two elliptical lobes, the pad in Bronze and Steel shaft. The geometrical

characteristics of the bearing and the operating conditions and the parameters of the lubricant specified in Table1.

Bearing length	$L_{ell} = 75mm$
Bearing length	$L_{cyl} = 75mm$
Length/Diameter	$L_{cyl}/D_{cyl}=0.57$
Outer radius of the bearing	$R_{ext} = 72mm$
Inside radius of the bearing	$R_{int} = 65mm$
shaft radius	$R_a = 45mm$
Young's modulus	$E_c = 12e^{+10}Pa$
Poisson coefficient	$\nu_c = 0.33$
Thermal conductivity of bushing	$K_{hc} = 50W/m.K$
Thermal conductivity of shaft	$K_{ha} = 75W/m.K$
Lubricant viscosity	$\mu_0 = 0.02068Pa.s$
Density of lubricant	$\rho = 869.53Kg.m^3$
Specific heat of lubricant	$C_p = 2000J.Kg.K$
Thermal conductivity of lubricant	$K_h = 0.13W/m.k$
Supply pressure	$P_0 = 1MPa$
Supply temperature	$T_0 = 300K$
Rotation speed	$1000 \leq \omega \leq 4000rpm$
Eccentricity	$20\mu m \leq e \leq 80\mu m$

TABLE1: The geometrical characteristics of the bearing (cylindrical and elliptical), lubricant and operating conditions

Relative difference	Convergence criterion
$\Delta P/P$	10^{-6}
$\Delta T/T$	10^{-6}
$\Delta h/h$	10^{-4}
$\Delta u/u, \Delta v/v, \Delta w/w$	10^{-2}

TABLE2: Convergence criteria

A. Results CFD and FSI

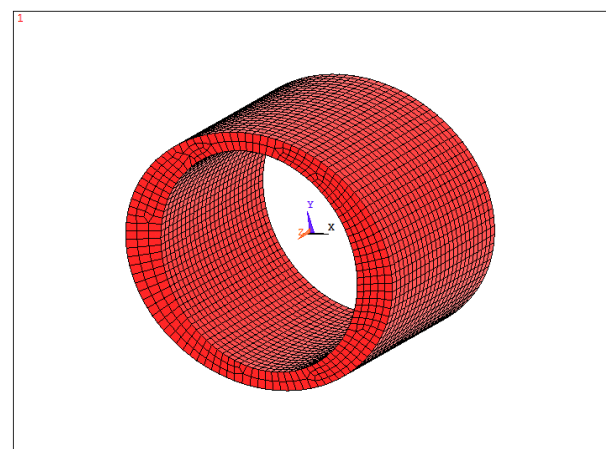


Figure1: Mesh film lubricant (11910 nodes) elliptical bearing.

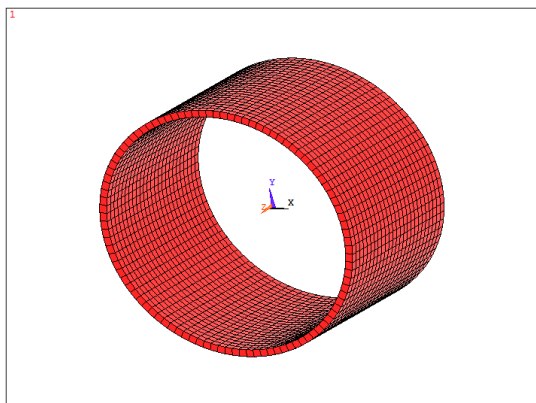


Figure2: Mesh of bearing (5200 nodes) elliptical bearing.

Figure3 respectively each have the three-dimensional field distribution of pressure and temperature in the lubricating film for a rotation speed of tree 2000rpm and an initial eccentricity $20\mu\text{m}$. It is observed, that the fields of temperature and pressure is commonly divided into the circumferential direction, and they reach its maximum axial. Thus respectively order of 18.2MPa and 330K. More pressure and temperature attained its maximum in the lobes of the bearing ($\theta=-90^\circ$ and $\theta=90^\circ$).

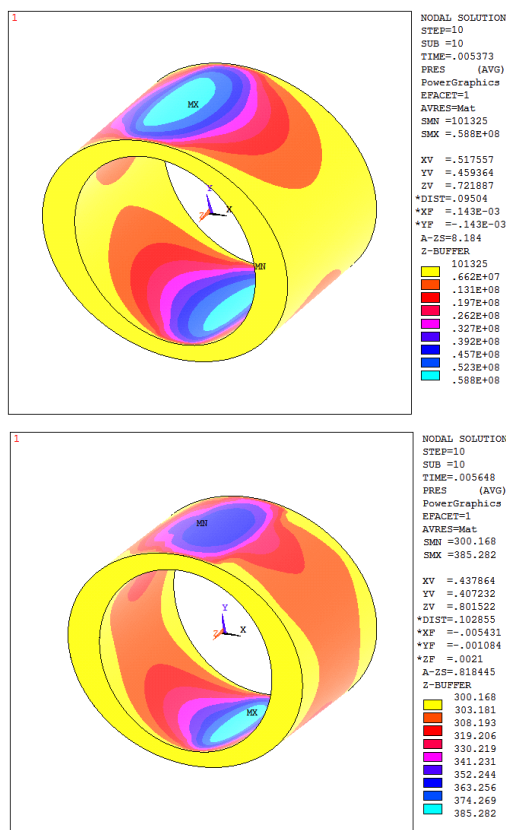


Figure3: The 3D field distribution of temperature and pressure in the lubricant film

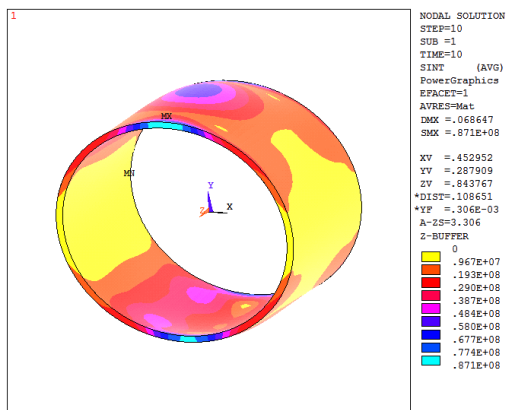
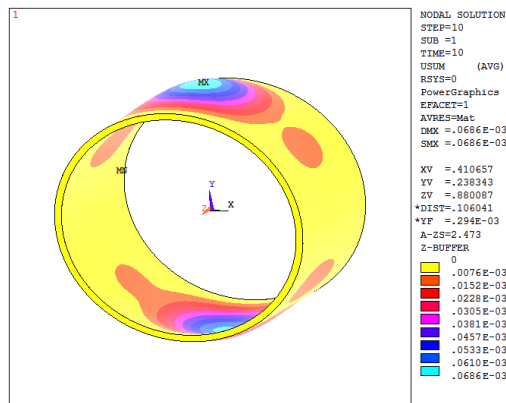


Figure4: The 3D field distribution of displacement and stress of the bearing

Figure4 have the three-dimensional distribution of displacement fields respectively U_{sum} and S_{sum} in the bush. Under the effect of the field of pressure and temperature, deforms the pad, to a greater extent in the median plane of which the thickness of the lubricant film is minimal. It may be noted that the stress peaks in the downstream of the area where the lubricant film thickness is minimal, which corresponds to the area of displacement U_{sum} Maximum pad, especially at the ends $Z=\pm L/2$. The displacement field peaked in the lobes, order $U_{max}=68,4\mu\text{m}$. The stress reaches its maximum value $S_{max}=87.1\text{ MPa}$ in the ends $Z=\pm L/2$. This is due to made that, at these ends; the installation (a boundary condition) generates significant constraints.

IV. PARAMETRIC STUDY

In this part we are interested in studying the influence of the rotational speed on the field of pressure, temperature displacement and stress intensity in the middle ($z=0$ and $0^\circ \leq \theta \leq 360^\circ$).

A. The influence of the speed on performance TEHD

Figure5 expose the influence of the rotational speed on the field of pressure and temperature as a function of the angular coordinate in the median plane of the bearing. An increase in pressure around 5.29% of $\omega_1=1000\text{rpm}$ and $\omega_4=4000\text{rpm}$ and an increase of order 8.22% for temperature is observed.

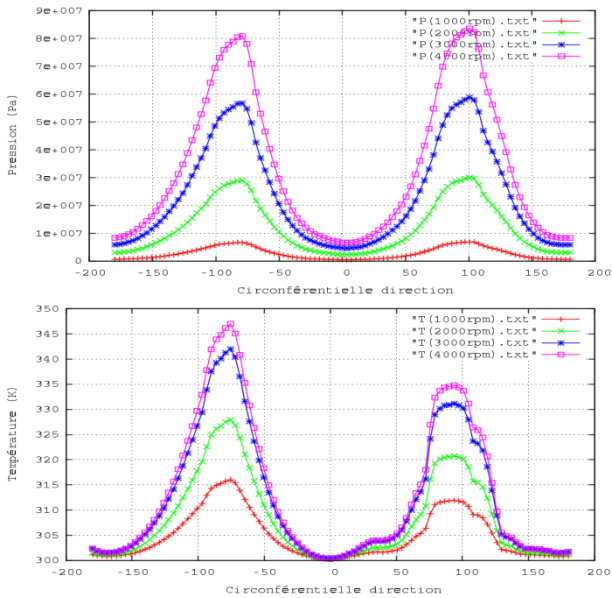


Figure5: Circumferential distribution of fields P and T for different values of ω

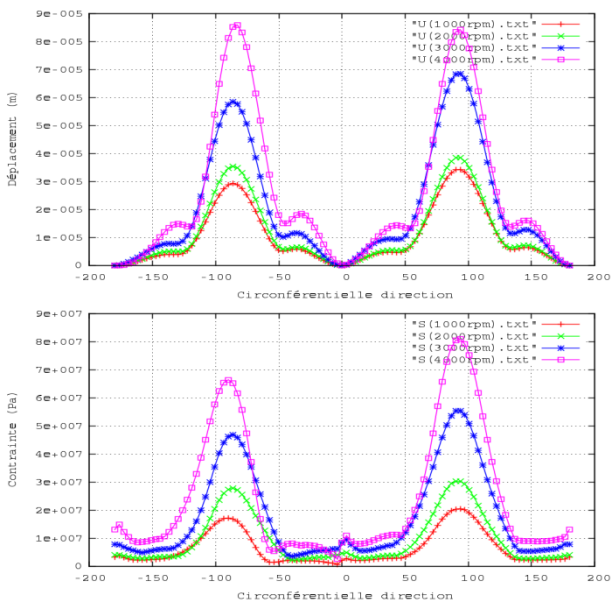


Figure6: Circumferential distribution of fields U and S for different values of ω

Figure6 shows the influence of the rotation speed of the circumferential distribution of the displacement field U and the stress S in the bearing inner surface. For a speed of 1000rpm was $U_{max}=34.3\mu m$ and $S_{max}=20.5 MPa$ and 4000rpm found $U_{max}=86\mu m$ and $S_{max}=81MPa$ therefore the displacement field and stress acceded respectively an increase of around 60% and 63%.

B. The influence of eccentricity on performance TEHD

In Figure7 we see that there is an asymmetry in the field distribution of pressure and temperature. For an eccentricity $20\mu m$ pressure and temperature reached their maximum values $P_{max}=25.9MPa$ $T_{max}=308K$ and an eccentricity $80\mu m$ pressure and temperature to $P_{max}=68.1MPa$ $T_{max}=341K$ by finding the two variables respectively underwent an elevation of about 38% and 10.41%.

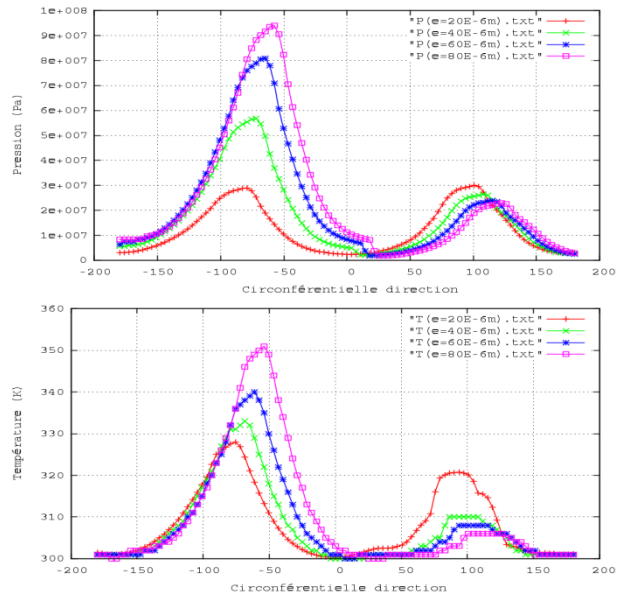


Figure7: Circumferential distribution of fields P and T for different values of eccentricity

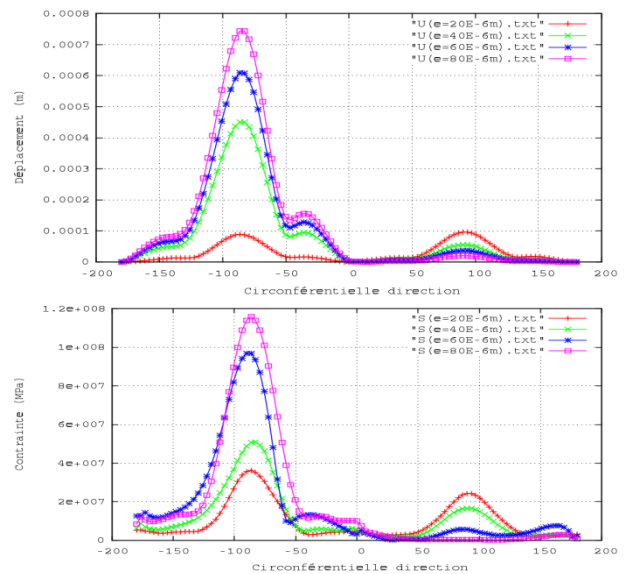


Figure8: Circumferential distribution of fields U and S for different values of eccentricity

The influence of eccentricity on the displacement field U and the constraint S is presented respectively in Figure8.

The displacement field has reached a maximum value of $96.20\mu m$ for eccentricity $20\mu m$ and eccentricity $80\mu m$ reached a maximum value of $744\mu m$, an increase was observed significant order 87.07%. Regarding stress, there is an increase of the maximum order value 70.50% between the eccentricity $20\mu m$ $S_{max}=36.2MPa$ and $80\mu m$ $S_{max}=116MPa$.

	$\Delta P(MPa)$	$\Delta T(K)$	$\Delta U(MPa)$	$\Delta S(MPa)$
$\omega 1=1000rpm$; $e3=60\mu m$	2.55	17.69	111	235
$\omega 1=2000rpm$; $e3=60\mu m$	12.56	27.99	131	274
$\omega 1=3000rpm$; $e3=60\mu m$	27.6	44.98	149	326
$\omega 1=4000rpm$; $e3=60\mu m$	48.2	56.98	165	351

Table3: The influence of speed " ω " on strained $\Delta P(MPa)$, $\Delta T(K)$, $\Delta U(MPa)$ and $\Delta S(MPa)$ a cylindrical bearing.

	ΔP (MPa)	ΔT (K)	ΔU (MPa)	ΔS (MPa)
$\omega_1=2000\text{rpm}; e_3=20\mu\text{m}$	8.34	18.12	46.2	94.77
$\omega_1=2000\text{rpm}; e_3=40\mu\text{m}$	9.22	22	54.7	100.32
$\omega_1=2000\text{rpm}; e_3=60\mu\text{m}$	12.65	27.99	131	273.83
$\omega_1=2000\text{rpm}; e_3=80\mu\text{m}$	17.4	34	154	297.67

Table4: The influence of eccentricity “e” on strained ΔP (MPa), ΔT (K), ΔU (MPa) and ΔS (MPa) a cylindrical bearing.

	ΔP (MPa)	ΔT (K)	ΔU (MPa)	ΔS (MPa)
$\omega_1=1000\text{rpm}; e_3=20\mu\text{m}$	6.37	15.57	34.3	19.4
$\omega_1=2000\text{rpm}; e_3=20\mu\text{m}$	27.68	25.47	38.5	28.1
$\omega_1=3000\text{rpm}; e_3=20\mu\text{m}$	54.17	41.51	68.6	51.9
$\omega_1=4000\text{rpm}; e_3=20\mu\text{m}$	77.10	46.70	86.0	78.4

Table5: The influence of speed “ ω ” on strained ΔP (MPa), ΔT (K), ΔU (MPa) and ΔS (MPa) an elliptical bearing.

	ΔP (MPa)	ΔT (K)	ΔU (MPa)	ΔS (MPa)
$\omega_1=2000\text{rpm}; e_3=20\mu\text{m}$	27.68	25.47	38.5	28.1
$\omega_1=2000\text{rpm}; e_3=40\mu\text{m}$	54.71	32.86	45.1	50.26
$\omega_1=2000\text{rpm}; e_3=60\mu\text{m}$	79.04	39.78	60.9	96.7
$\omega_1=2000\text{rpm}; e_3=680\mu\text{m}$	92.19	50.7	74.4	115.29

Table6: The influence of eccentricity “e” on strained ΔP (MPa), ΔT (K), ΔU (MPa) and ΔS (MPa) an elliptical bearing.

Presenting in Figures 9, 10, 11 and 12 curves that allow us to provide an overall summary of the influence of the rotational speed and eccentricity variations on extended ΔP (MPa), ΔT (K), ΔU (MPa) and ΔS (MPa) for two geometries treated, cylindrical and elliptical. See Tables 3, 4, 5 and 6.

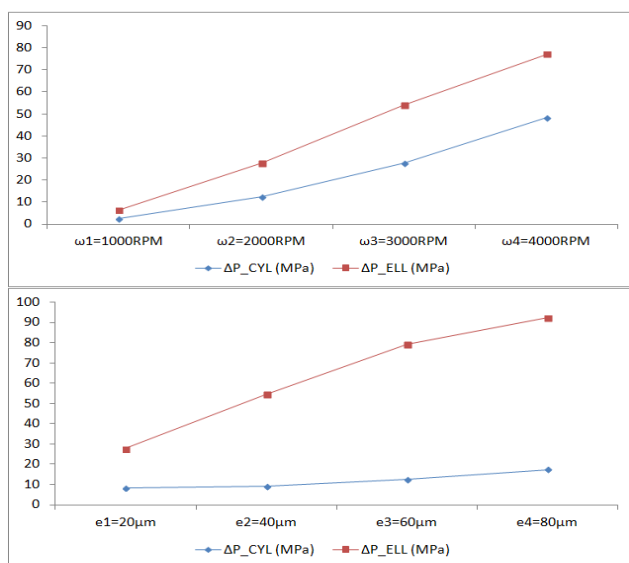


Figure9: The influence of the rotational speed and eccentricity of ΔP (MPa) for both elliptical and cylindrical geometries.

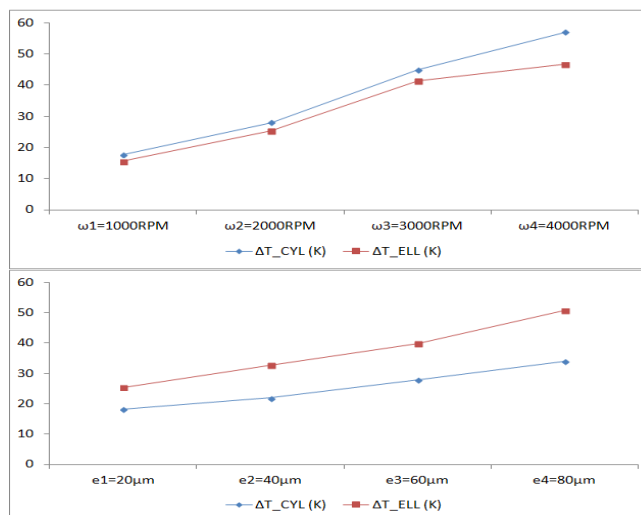


Figure10: The influence of the rotational speed and eccentricity of ΔT (MPa) for both elliptical and cylindrical geometries.

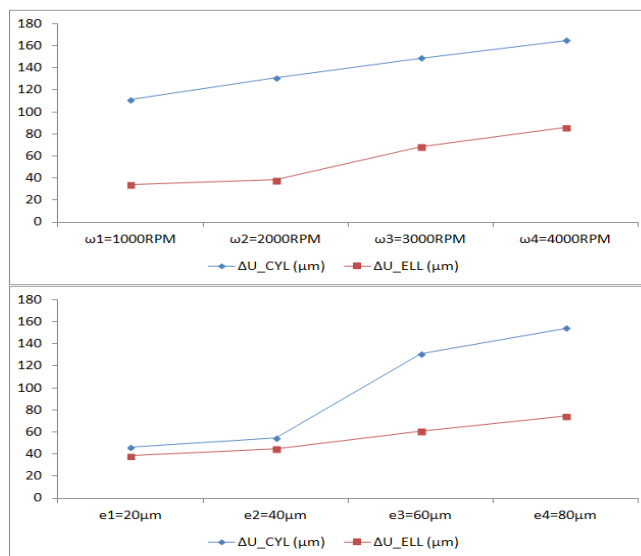


Figure11: The influence of the rotational speed and eccentricity of ΔU (MPa) for both elliptical and cylindrical geometries.

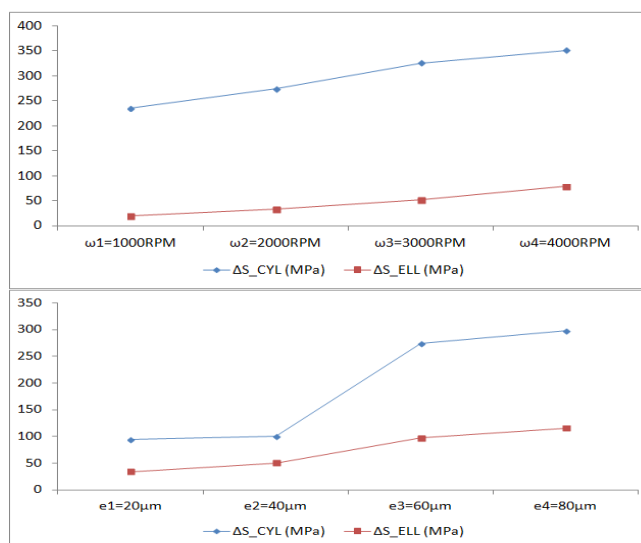


Figure12: The influence of the rotational speed and eccentricity of ΔS (MPa) for both elliptical and cylindrical geometries.

Whatever the operating conditions and the geometrical characteristics of the bearing, it can be concluded that the hydrodynamic performance trends obtained through the two geometries are the same.

Figure 9 shows that the pressure values at the elliptical bearing are greater than those of the cylindrical bearing, for different values of eccentricity and the rotation speed. While the temperature values for the elliptical bearing are less than those of the cylindrical bearing figure 10, for different values of eccentricity and the rotation speed.

Despite the significant values of the pressure field for the elliptical bearing compared to the cylindrical bearing, we see that the displacement values at the elliptical bearing for eccentricity 20 μm and with different values of speed are lower. This shows the advantage of the geometric shape of the elliptical bearing when the rotational speed varies figure 11. Unlike the influence of rotational speed on the displacement, that shows the influences of the eccentricity on the maximum displacement values are greater for the elliptical bearing.

V. CONCLUSION

This paper has studied the nonlinear analysis of lubrication "TEHD" a cylindrical and elliptical bearing (two lobes). Using one hand, the numerical simulation Computational Fluid Dynamic "CFD" which allowed us to determine the pressure field and temperature in the lubricant film. On the other hand we used another Fluid Structure Interaction numerical simulation "FSI" to calculate the displacement field and the stress in the bearing. It should be noted, however, that the conclusions we give in this article are valid only for the specific cases that we studied, and they are not independent of the characteristics of the bearing and lubricant. Our work must be completed to show the influence of material properties and lubricant as well as the dimensions of the bearing elements in determining its performance.

REFERENCES

- [1] B.S.Shenoy, R.S.Pai, D.S.Rao and R.Pai 2009 Elasto-hydrodynamic lubrication analysis of full 360° journal bearing using CFD and FSI techniques. World Journal of Modelling and Simulation 4 315-320.
- [2] Prabhakaran Nair K., Sukumaran Nair V.P. and Jayadas N.H. 2006 "Static and dynamic analysis of elastohydrodynamic elliptical journal bearing with micropolar lubricant", Tribology International 40, pp. 297-305.
- [3] A. Chauhan, R. Sehgal and R.K. Sharma 2010 Thermohydrodynamic analysis of elliptical journal bearing with different grade oils. Journal of Tribology International 43 1970-1977.
- [4] M.V. Phalle, S.C. Sharma and S.C. Jain 2011 Influence of wear on the performance of a 2-lobe multirecess hybrid journal bearing system compensated with membrane restrictor. Journal of Tribology International 44 380-395.
- [5] A. Kabouya and M. Lahmar and B. Bou-Said 2008 "Etude des paliers lisses mis en alignés lubrifiés par des huiles à couple de contrainte. Mécanique & Industries 8 577-595.
- [6] G. Adiletta, E. Mancusi and S. Strano 2011 Nonlinear behavior analysis of a rotor on two-lobe wave journal bearings. Journal of Tribology International 44 42-54.
- [7] A. Ouadoud, A. Mouchtachi and N. Boutammachte 2011 Numerical simulation CFD, FSI of a hydrodynamic journal bearing. Journal of Advanced Research in Mechanical Engineering 2 33-38.
- [8] J. Bouyer and M. Fillon 2000 Experimental study on thermal effects of a misaligned hydrodynamic journal bearing. 7th Portuguese Conference on Tribology Porto, Portugal 76 63-66.
- [9] A. Ouadoud, A. Mouchtachi and N. Boutammachte 2013 Numerical analysis of thermoelastohydrodynamic behavior of an elliptical two-lobe bearing. International Journal Advanced Materials 787 786-791
- [10] M.V. Phalle, S.C. Sharma and S.C. Jain 2011 Influence of wear on the performance of a 2-lobe multirecess hybrid journal bearing system compensated with membrane restrictor. Journal of Tribology International 44 380-395
- [11] Shenoy B.S., Pai R.S., Rao D.S. and Pai R. 2009 "Elasto-hydrodynamic lubrication analysis of full 360° journal bearing using CFD and FSI techniques", World journal of modeling and simulation, 5, pp. 315-320
- [12] Wang Y, Zhang C, Liu G, Wang J.Q. and Lin, C. 2001 "A mixed-TEHD analysis and experiment of journal bearing under severe operating conditions" .2nd World Tribology Congress. Vienne, Autriche 3-7 September
- [13] Ouadoud A., Boutammachte N. and Mouchtachi A. 2011 "Numerical simulation CFD, FSI of a hydrodynamic journal bearing", Journal of Advanced Research in Mechanical Engineering (JARME). Vol.2-Iss.1, pp. 33-38

First Author Pr. OUADOUD Aziz, PhD in Mechanical Engineering Tribology specialty, Professor of Higher Education assistant.